The rubber tree kinome: genome-wide characterization and insights into coexpression patterns associated with abiotic stress responses

Lucas Borges dos Santos[a,*], Alexandre Hild Aono[a,*], Felipe Roberto Francisco[a], Carla Cristina da Silva[a], Livia Moura Souza[a,b], Anete Pereira de Souza[a,c,**]

[a] *Molecular Biology and Genetic Engineering Center (CBMEG), University of Campinas (UNICAMP), Campinas, Brazil*

[b] *São Francisco University (USF), Itatiba, Brazil*

[c] *Department of Plant Biology, Biology Institute, University of Campinas (UNICAMP), Campinas, Brazil*

*The authors contributed equally

**Corresponding author

Email addresses: lucas.borgesst@gmail.com (Lucas Borges dos Santos), alexandre.aono@gmail.com (Alexandre Hild Aono), felipe.roberto.francisco@gmail.com (Felipe Roberto Francisco), silvacbio@yahoo.com.br (Carla Cristina da Silva), livia.souza@usf.edu.br (Livia Moura Souza), anete@unicamp.br (Anete Pereira de Souza)

Abstract

The protein kinase (PK) superfamily constitutes one of the largest and most conserved protein families in eukaryotic genomes, comprising core components of signaling pathways in cell regulation. Despite its remarkable relevance, only a few kinase families have been studied in *Hevea brasiliensis*. A comprehensive characterization and global expression analysis of the PK superfamily, however, is currently lacking. In this study, we identified and characterized the entire set of PKs, also known as the kinome, present in the Hevea genome. A total of 1,809 PK genes were identified using the current reference genome assembly at the scaffold level, and 1,379 PK genes were identified using the latest chromosome-level assembly and combined into a single set of 2,842 PKs. These proteins were further classified into 20 different groups and 122 families, exhibiting high compositional similarities among family members and with two phylogenetically close species (*Manihot esculenta* and *Ricinus communis*). Different RNA-sequencing datasets were employed to identify tissue-specific expression patterns and potential correspondences between different rubber tree genotypes. In addition, coexpression networks under several abiotic stress conditions, such as cold, drought and latex overexploitation, were employed to elucidate associations between families and tissues/stresses. Through the joint investigation of tandemly duplicated kinases, transposable elements, gene expression patterns, and coexpression events, we provided insights into the understanding of the cell regulation mechanisms in response to several conditions, which can often lead to a significant reduction in rubber yield.

Keywords: Coexpression networks, *Hevea brasiliensis*, kinase family, RNA-Sequencing, tandem duplications, transposable elements

1. Introduction

Rubber is one of the world's major commodities and is extensively used in various industrial and domestic applications, yielding more than 40 billion dollars annually (Board, 2018). The major source of latex for rubber production is *Hevea brasiliensis* (Hbr), commonly referred to as rubber tree, a perennial native plant from the Amazon rainforest belonging to the *Euphorbiaceae* family (Priyadarshan and Goncalves, 2003). Although the warm and humid weather in the Amazon region offers a favorable climate for Hbr growth and propagation, large-scale cultivation of Hbr is unviable due to the incidence of a highly pathogenic fungus, *Pseudocercospora ulei* (Hora Júnior et al., 2014). Thus, rubber tree plantations were transferred to other countries and regions, which could not offer optimal conditions for the development of tropical crops due to the low temperatures during winter, dry periods, and elevated wind incidence (Hoa et al., 1998). Exposure to these new abiotic stresses often leads to a significant reduction in latex production in most Hbr wild varieties, which has stimulated the development of breeding programs with a focus on stress-tolerant cultivars (Priyadarshan and Goncalves, 2003; Pushparajah, 1983).

Different types of abiotic stresses may trigger several physiological responses in susceptible rubber tree genotypes and often impact their survival, growth and productivity, depending on the age and vigor of the affected plant (Kuruvilla et al., 2017). In general, cold and drought stresses result in the inhibition of photosynthesis and chlorophyll degradation (Devakumar et al., 2002). Water deficit may affect the plant growth and canopy architecture of trees, and its impact during tapping seasons tends to be more severe due to the deviation of resources (carbon and water) caused by wounding stress (Devakumar et al., 1999; Kunjet et al., 2013). Cold damage leads to a decrease in membrane permeability (Meti et al., 2003; Sevillano et al., 2009), together with photosynthesis inhibition, causing more critical injuries to the plant, such as the wilting and yellowing of leaves, interveinal chlorosis, darkening of the green bark, reduction of latex flow and dieback of shoots (Meti et al., 2003).

The ability to sense and adapt to adverse conditions relies on the activation of complex signaling networks that protect plants from potential damage caused by these environmental changes (Kovtun et al., 2000). Protein kinases (PKs) comprise one of the most diverse protein superfamilies in eukaryotic organisms (Liu et al., 2015) and act as key components in stimulus

perception and signal transduction through a chain of phosphorylation events, resulting in the activation of genes and several cellular responses (Colcombet and Hirt, 2008). The expansion of this family underlies several mechanisms of gene duplication throughout the evolutionary history of eukaryotes, including chromosomal and whole-genome duplication, tandem duplication in linked regions and retroposition events, leading to more specialized or novel gene functions (Zhang, 2003).

In the rubber tree, several kinase families have been characterized, including the mitogen-activated protein kinase (MAPK) (Jin et al., 2017), calcium-dependent protein kinase (CDPK) (Xiao et al., 2017; Zhu et al., 2018b), CDPK-related protein kinase (CPK) (Xiao et al., 2017), and sucrose non-fermenting 1-related protein kinase 2 (SnRK2) (Guo et al., 2017). These studies revealed contrasting expression patterns of the kinase families among tissues, in addition to the elevated expression of the SnRK2 and CPK families in laticifers in response to ethylene, ABA, and jasmonate stimulation (Guo et al., 2017; Zhu et al., 2018b), suggesting their potential participation during several developmental and stress-responsive processes. However, the comprehensive identification and characterization of rubber tree PKs has not yet been performed and would greatly benefit plant science research to promote a better understanding of the molecular mechanisms underlying the stress response.

In this study, we investigated the kinase diversity present in the Hbr genome through a thorough characterization of its PKs, including the subfamily classification and the prediction of several protein properties, such as molecular weight, subcellular localization, and biological functions. The rubber tree kinome, defined as the complete repertoire of PKs, was estimated using a combined analysis with the two major genome assemblies of rubber tree and comparative analyses with cassava (*Manihot esculenta* (Mes)) and castor plant (*Ricinus communis* (Rco)) kinomes. Furthermore, RNA sequencing (RNA-Seq) data from different Hbr genotypes were used to identify expression patterns of the kinase subfamilies, followed by the construction of gene coexpression networks for control and abiotic stress conditions. Our study provides broad resources for future functional investigations and valuable insights into the major components associated with cell adaptation in response to environmental stresses.

2. Material and methods

2.1. Data acquisition

Sequence and annotation files of Hbr, Mes, and Rco were downloaded from the NCBI (Geer et al., 2010) and Phytozome v.13 (Goodstein et al., 2012) databases. We selected the latest genomes of cassava v.7.1 (Bredeson et al., 2016) and castor plant v.0.1 (Chan et al., 2010), as well as two major genomes of the rubber tree: the latest chromosome-level genome (Liu et al., 2020b) (Hb_chr) and the reference scaffold-level assembly (Tang et al., 2016) (Hb_scaf), under accession numbers PRJNA587314 and PRJNA310386 in GenBank, respectively. The same data analysis procedures for PK identification and characterization were applied to Hbr, Mes and Rco.

2.2. Kinome Definition

The hidden Markov models (HMMs) of the two typical kinase domains, Pkinase (PF00069) and Pkinase_Tyr (PF07714), were retrieved from the Pfam database (El-Gebali et al., 2019). To select putative proteins having one or more kinase domains, protein sequences were aligned to each HMM profile using HMMER v.3.3 (Finn et al., 2011) (E-value of 1.0E-10). We retained only sequences covering at least 50% of the respective domain and the longest isoform.

The Hbr kinome was created as a combination of putative PKs identified from two different genomic datasets: Hb_chr and Hb_scaf. To avoid redundancy, we combined the sets using CD-HIT v.4.8.1 software (Fu et al., 2012) with the following selection criteria: (i) for proteins present in both sets as a single copy, the longest sequence was retained, and the other one was discarded; and (ii) when putative duplications were present, i.e., there were protein clusters with significant similarities in both Hb_chr and Hb_scaf, and all proteins from the largest set were retained. For pairwise comparisons, we set a minimum sequence identity threshold of 95% and a maximum length difference of 75%.

2.3. Kinase characterization and phylogenetic analyses

The PKs were classified into groups and subfamilies according to the HMMs of each family built from four plant model species (*Arabidopsis thaliana*, *Chlamydomonas reinhardtii*, *Oryza sativa*, and *Physcomitrella patens*) and supported among 21 other plant species (Lehti-Shiu

and Shiu, 2012). The classification was further validated through phylogenetic analyses. The domain sequences from all PKs were aligned using Muscle v.8.31 (Edgar, 2004), and a phylogenetic tree was constructed for each kinase dataset using the maximum likelihood approach in FastTree v.2.1.10 software (Price et al., 2010) with 1,000 bootstraps and default parameters through CIPRES gateway (Miller et al., 2011). The resulting dendrograms were visualized and plotted using the statistical software R (Ihaka and Gentleman, 1996) together with the ggtree (Yu et al., 2017) and ggplot2 (Villanueva and Chen, 2019) packages.

For each PK, we obtained the following characteristics: (a) gene location and intron number, according to the GFF annotation files; (b) molecular weight and isoelectric point with ExPASy (Gasteiger et al., 2003); (c) subcellular localization prediction using CELLO v.2.5 (Yu et al., 2006) and LOCALIZER v.1.0.4 (Sperschneider et al., 2017) software; (d) the presence of transmembrane domains using TMHMM Server v.2.0 (Krogh et al., 2001); (e) the presence of N-terminal signal peptides with SignalP Server v.5.0 (Armenteros et al., 2019); and (f) gene ontology (GO) term IDs using Blast2GO software (Conesa and Götz, 2008) together with the SwissProt Viridiplantae protein dataset (Consortium, 2019).

2.4. Duplication events in the rubber tree kinome

We determined duplication events of the PK superfamily in Hbr based on the physical location of PK genes and their compositional similarities assessed through comparative alignments with the Hbr genome using the BLASTn algorithm (Altschul et al., 1990). Tandem duplications were defined as PK pairs separated by a maximum distance of 25 kb on the same chromosome and with the following: (i) a minimum similarity identity of 95%; (ii) an E-value cutoff of 1.0E-06; and (iii) a 75% minimum sequence length coverage. The chromosomal location of putative tandemly duplicated PK genes was illustrated using MapChart v.2.32 (Voorrips, 2002), and synteny relationships of the PKs were visualized using Circos software v.0.69 (Krzywinski et al., 2009).

2.5. Transposable element search

We searched for transposable elements (TEs) in the Hbr genome using TE data of 40 plant species obtained from the PlanNC-TE v3.8 database (Pedro et al., 2018). For this purpose, we

performed a comparative alignment between the TEs retrieved and the *H. brasiliensis* reference chromosomes using BLASTn (Altschul et al., 1990) for short sequences (blastn-short) with the following parameters: (i) minimum coverage of 75%; (ii) word size of 7; and (iii) an E-value cutoff of 1.0E-10. We selected TEs located within a 100 kb window from Hbr PK genes. The chromosomal localization of TEs was illustrated using MapChart v.2.32 (Voorrips, 2002).

2.6. RNA-Seq data collection

Several publicly available Hbr RNA-Seq experiments were collected from the NCBI Sequence Read Archive (SRA) database (Leinonen et al., 2010). The samples consisted of a wide range of tissues and comprised various genotypes. In total, we obtained 129 samples from 10 studies (Cheng et al., 2018; Deng et al., 2018; Lau et al., 2016; Li et al., 2016; Mantello et al., 2019; Montoro et al., 2018; Rahman et al., 2019; Sathik et al., 2018; Tan et al., 2017; Tang et al., 2016) that evaluated control and stress conditions (cold, drought, latex overexploitation, jasmonate, and ethylene treatments).

2.7. Expression analysis

The raw sequence data were submitted to a sequence quality control assessment using the FastQC tool (Andrews, 2010), following a low-quality read filtering and adapter removal step using Trimmomatic software v.0.39 (Bolger et al., 2014). After removing adapter sequences, we retained only reads larger than 30 bp and bases with Phred scores above 20. The corresponding coding sequences (CDSs) from Hb_chr and Hb_scaf were used as a reference for the quantification step using Salmon software v.1.1.0 (Patro et al., 2017) with the k-mer length parameter set to 31. The expression values of each PK transcript were normalized using the transcript per million (TPM) metric, and samples containing biological replicates were combined by defining the mean value among replicates. To visualize the expression of each kinase subfamily among different tissues and cultivars, we generated two heatmap figures for control and stressed samples using the R package pheatmap (Kolde and Kolde, 2015).

2.8. Coexpression network construction

Two coexpression networks of Hbr PK subfamilies, corresponding to control and abiotic stress situations, were modeled and visualized using the R package igraph (Csardi et al., 2006)

with the minimum Pearson correlation coefficient set to 0.7. To assess the structure of each network and specific subfamily attributes, we estimated the hub scores of each PK subfamily from Kleinberg's hub centrality scores (Kleinberg, 1999) and edge betweenness values from the number of geodesics passing through each edge (Brandes, 2001).

3. Results

3.1. Genome-wide identification, classification and characterization of PKs

Based on the established pipeline, we identified 2,842 typical putative PK genes in Hbr (Supplementary Table S1a), 1,531 in Mes (Supplementary Table S1b), and 863 in Rco (Supplementary Table S1c). The rubber tree kinome resulted from a combination of 1,206 (42.43%) proteins from the Hb_scaf dataset and 1,636 (57.57%) from Hb_chr. Interestingly, we also identified several PKs containing multiple kinase domains in all three datasets (191, 91, and 44 in Hbr, Mes and Rco, respectively) (Supplementary Tables S2). Typical PKs were defined as protein sequences presenting high similarity to a given kinase domain with minimum coverage of 50%. The atypical PKs of Hbr (728), Mes (230), and Rco (95) were removed from subsequent analyses.

Typical Hbr, Mes, and Rco PKs were further classified into groups and subfamilies based on the HMM profiles of 127 kinase subfamilies defined by Lehti-Shiu and Shiu (2012). The PK domain classification was validated by phylogenetic analyses (Supplementary Figs. S1-S2). Thus, PKs were grouped into 20 major groups: PKs A, G and C (AGC), Aurora (Aur), budding uninhibited by benzimidazoles (BUB), calcium- and calmodulin-regulated kinases (CAMK), casein kinase 1 (CK1), cyclin-dependent, mitogen-activated, glycogen synthase, and CDC-like kinases (CMGC), plant-specific, inositol-requiring enzyme 1 (IRE1), NF-kB-activating kinase (NAK), NIMA-related kinase (NEK), Pancreatic eIF-2α kinase (PEK), Receptor-like kinase (RLK)-Pelle, *Saccharomyces cerevisiae* Scy1 kinase (SCY1), Serine/threonine kinase (STE), Tyrosine kinase-like kinase (TKL), Tousled-like kinases (TLK), Threonine/tyrosine kinase (TTK), Unc-51-like kinase (ULK), Wee1, Wee2, and Myt1 kinases (WEE), and with no lysine-K (WNK). We also identified 72 PKs in Hbr (2.5%), 30 in Mes (2.0%), and 22 in Rco (2.5%) that did not cluster in accordance with any subfamily classification and were placed in the "Unknown"

category (Supplementary Tables S3).

The RLK-Pelle was the most highly represented group in all three species, as evidenced in Fig. 1, and was divided into 59 different subfamilies, accounting for 65.5%, 68.1%, 65.2% of all rubber tree, cassava, and castor plant PKs, respectively, followed by the CMGC (6.4% in Hbr, 5.9% in Mes, 7.5% in Rco), CAMK (5.9% in Hbr, 6.5% in Mes, 6.5% in Rco), TKL (4.9% in Hbr, 4.9% in Mes, 5.6% in Rco) and others (Supplementary Table S4).

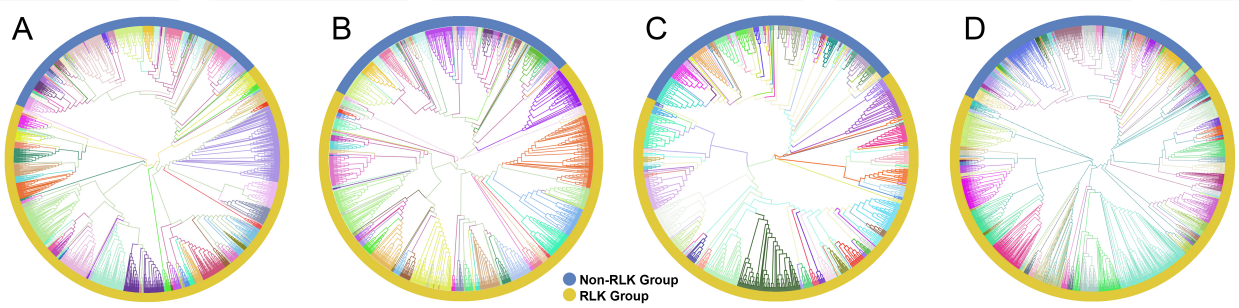

Fig. 1. Phylogenetic analyses of putative typical protein kinases (PKs) identified in the *Hevea brasiliensis* (Hbr), *Manihot esculenta* (Mes), and *Ricinus communis* (Rco) genomes. (A) Phylogenetic tree constructed with 2,842 Hbr PKs organized into 123 subfamilies. (B) Phylogenetic tree of the 1,531 Mes PKs organized into 123 subfamilies. (C) Phylogenetic tree of the 863 Rco PKs organized into 125 subfamilies. (D) Phylogenetic tree of all Hbr, Mes, and Rco PKs. Kinase subfamilies are represented by different branch colors.

We investigated the chromosomal positions, intron distribution and structural properties of Hbr, Mes, and Rco PKs using several approaches (Supplementary Tables S5-S7). Hbr and Mes PK genes were distributed along all Hbr and Mes chromosomes (Supplementary Fig. S3) with a higher concentration within the subtelomeric regions. Most PK genes contained at least 1 intron, and only 284 (10.0%), 229 (14.9%), and 140 (16.2%) intronless genes were found in Hbr, Mes, and Rco, respectively.

Most interestingly, the protein characteristics of all three kinomes were highly comparable. Several PKs had predicted transmembrane domains (45.6% in Hbr, 50.5% in Mes, and 48.2% in Rco) and N-terminal signal peptides (29.6%, 37.3%, and 33.5%, respectively). Similarly, the distribution of molecular weights and isoelectric points was relatively uniform (Supplementary Fig. S4). Moreover, the subcellular localization predictions performed with the selected software were mostly on the plasma membrane, cytoplasm and nucleus (Supplementary Fig. S5), in accordance with the enriched "cellular component" GO category (Supplementary Tables S8; Supplementary Fig. S5).

Finally, we investigated the domain composition of PKs based on the complete set of con-

served domains present in the Pfam database. In total, we identified 1,472 PKs containing additional conserved domains in Hbr (52.8%), 827 in Mes (54.0%) and 442 in Rco (51.2%) (Supplementary Tables S9-S10). Interestingly, this observation comprises a significant portion of members from groups CAMK (58.0% in Hbr, 61.6% in Mes, and 64.3% in Rco), RLK-Pelle (63%, 65.5%, and 63.9%, respectively), and TKL (48.2%, 48%, and 52%).

Kinase duplication events in H. brasiliensis

To examine the expansion of PK subfamilies, tandemly duplicated kinase genes were identified based on their physical localization on Hbr chromosomes, and protein similarities were assessed through comparative alignments. Taken together, we found that 339 of the 2,842 Hbr PK genes (∼11.9%) were arranged in clusters of highly similar gene sequences among the 18 reference chromosomes, which are likely to represent tandem duplication events (TDEs) of the kinase superfamily in rubber tree (Fig. 2A). These genes were dispersed in 145 separate clusters and comprised members of 63 kinase subfamilies (Supplementary Tables S11-S12). Chromosome 14 showed the highest number of TDEs (19), containing 47 PK genes. In contrast, chromosome 1 contained the least number of TDEs (2). We found that for many kinase subfamilies, a large portion of their members originated from TDEs. A total of 100%, 100%, and 75% of TTK, ULK_Fused, and CMGC_CDKL-Os members were tandemly organized, while other subfamilies, such as RLK-Pelle_DLSV, showed the largest absolute number of TDEs (45) distributed across 9 chromosomes, although it accounted for only 16.8% (45/268) of its total size.

Segmental duplication events were estimated based on sequence similarities between two or more PKs separated by a genomic window larger than 100 kb or present in different chromosomes. Genomic correspondences increased as the sequence similarity decreased (Fig. 2D). In total, we identified 858 kinase correspondences with compositional similarity greater than 90%, 1,673 for 75% and 10,121 for 50%. To further investigate potential biological processes associated with duplicated kinase genes, we performed a functional annotation pipeline on tandemly duplicated PKs and selected GO terms related to the "biological process" category (Supplementary Fig. S6). The findings were very consistent with those resulting from the analysis performed using the complete set of Hbr PKs (Supplementary Fig. S7).

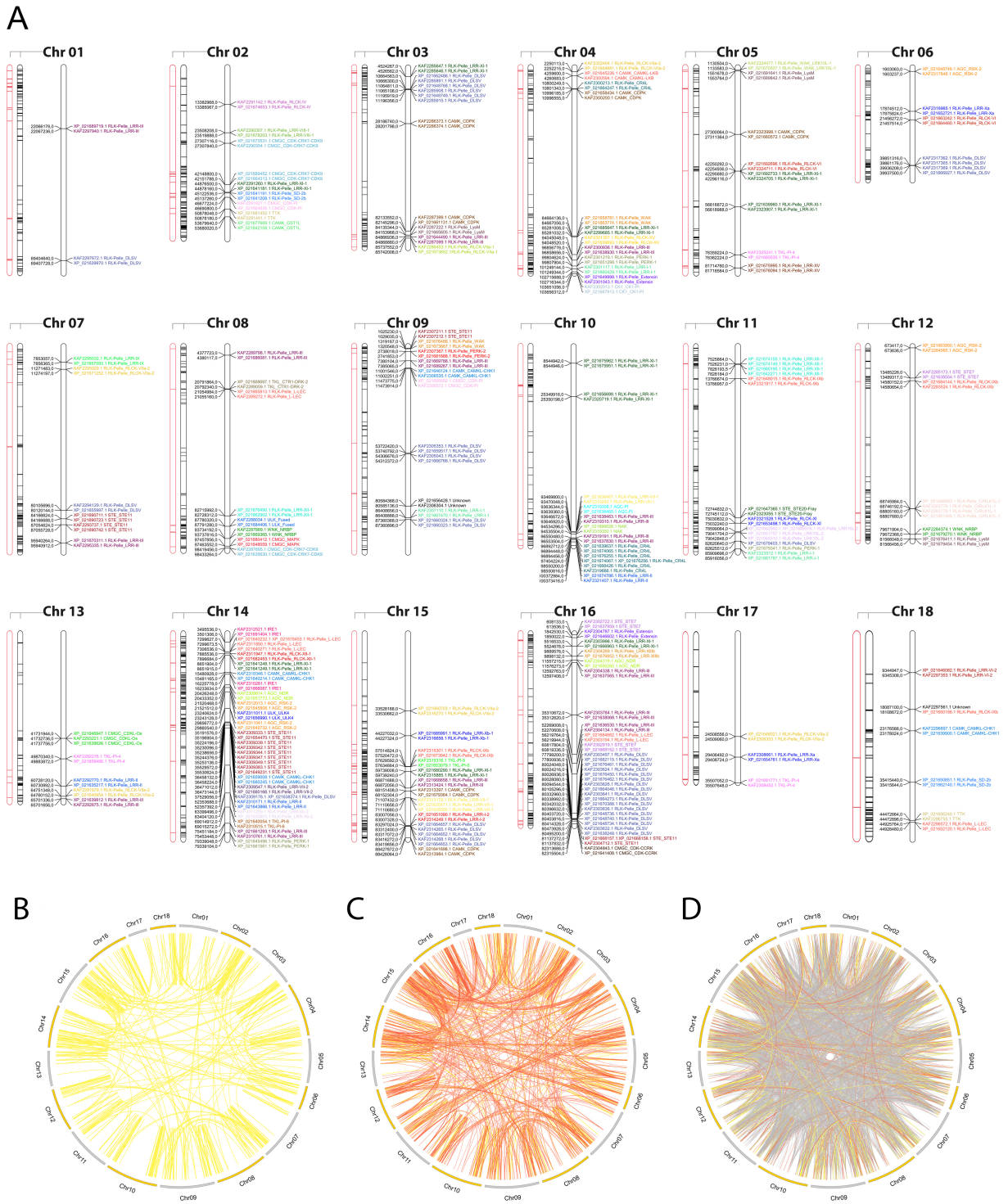

Fig. 2. (A) Kinase distribution along *Hevea brasiliensis* chromosomes. For each chromosome, from left to right: (i) transposable elements located within a 100 kb window around kinase genes are highlighted in red; (ii) all genes with kinase domains are highlighted in black; and (iii) tandemly duplicated kinase genes are colored and labeled according to the kinase subfamily classification. (B) Potential segmental duplication events in the *H. brasiliensis* genome considering similarities greater than 90% (yellow); (C) 75% (orange); and (D) 50% (gray).

Transposable elements in H. brasiliensis genome

We predicted TEs near Hbr PK genes using a comprehensive database that combined data from overlapping regions of TE features and several classes of noncoding RNAs (ncRNAs). Overall, the percentage of TEs associated with PK genes in the rubber tree was reduced (23.7%) when compared to overlapping ncRNAs (76.3%) (Supplementary Table S13). Out of the 8,457 annotated TEs in the reference genome, 88% were classified as long terminal repeat (LTR) retrotransposons. These elements appeared to be associated (within a 100 kb genomic window) with 362 (12.7%) kinase genes (Fig. 2A, Supplementary Table S14), of which 56 (15.5%) were tandemly duplicated. Nearly 73.2% of these duplicated genes were members of the RLK-Pelle group.

Expression patterns of PK subfamilies

We analyzed the expression levels of 118 kinase subfamilies among 129 samples related to control and different abiotic stress conditions (Supplementary Table S15). The resulting dataset comprised transcriptomic data of 14 different cultivars from a wide variety of tissues and organs, including leaf, petiole, bark, latex, seed, male and female flowers, in early and mature developmental stages. After filtering out low-quality reads and removing adapter sequences, we mapped the filtered reads to the complete set of CDS sequences in Hb_chr and Hb_scaf reference genomes separately and further generated a subset of the quantifications corresponding to PK genes present in the Hbr kinome. The results were normalized to TPM values (Supplementary Tables S16-S17), and 3 samples presenting significantly low quantifications were excluded (Hb_Bark_3001_normal_rep1, Hb_Latex_712_normal_rep2, Hb_Latex_2025_normal_rep1). For cases where replicates were present, the expression values were averaged.

For both control and stress heatmaps (Supplementary Figs. S8-S9, respectively), samples belonging to the same tissues were clustered together based on Euclidean distance measures. In general, we observed similar patterns of expression of each kinase subfamily within samples of a given tissue; however, specific experimental conditions of each RNA-Seq dataset may have influenced the expression levels, leading to inconsistent patterns in some cases. From left to right in the heatmap containing all experiments (Supplementary Fig. S10), there were 5 major

clusters separated into the following categories: (i) latex; (ii) leaf and seed tissues; (iii) bark, root, male and female flowers; (iv) leaf; and (v) samples from latex and petiole.

Interestingly, several subfamilies were highly expressed in nearly all samples, including AGC_PKA-PKG, TKL-Pl-1, RLK-Pelle_LRR-VIII-1, RLK-Pelle_RLCK-IXa, and Aur. Therefore, distinctions in PK expression between leaf and latex samples were clear. Latex and bark tissues presented lower expression in most subfamilies; however, we detected a few cases where the expression in latex and bark was significantly higher than that in leaves, such as STE_STE-Pl and RLK-Pelle_LRR-VIII-1. Additionally, we found a small number of subfamilies with elevated expression in bark (TKL-Pl-7 and ULK_ULK4), but we did not observe cohesive clustering of this tissue. Overall, in the analysis of the expression levels under abiotic stress conditions, the number of subfamilies that presented moderately high (dark orange) and high (red) expression apparently increased when compared to control samples (highlighted in blue).

Coexpression networks in response to abiotic stresses

The quantification analysis revealed different expression profiles of PK subfamilies among different tissues, genotypes and conditions. To expand our understanding of how these proteins interact under exposure to abiotic conditions, we further investigated potential relationships between kinase subfamilies by constructing coexpression networks based on the expression data described above. Using the Hbr PK set, two independent networks were constructed: one for control and one for abiotic stress conditions. For each network, we used the following conventions: (i) kinase subfamilies were represented by separate nodes; (ii) the node size corresponded to the mean gene expression value; (iii) the edges represented coexpression events determined by pairwise expression correlations between subfamilies with a minimum Pearson correlation coefficient of 0.7; and (iv) the edge thickness corresponded to the degree of correlation, from moderate (minimum PCC of 0.7) to fairly strong (minimum PCC of 0.9) correlations.

We observed a different number of edges between networks (1,162 in control and 704 in stress). Moreover, we found 15 elements in each network that were disconnected from the main core (i.e., kinase subfamilies with no significant correlation in expression); however, they were related to different subfamilies in each network (Fig. 3). Figs. 3B and 3D highlight the red

correlation similarities between control and stress coexpression networks, while edges in dark gray represent connections unique for each condition.

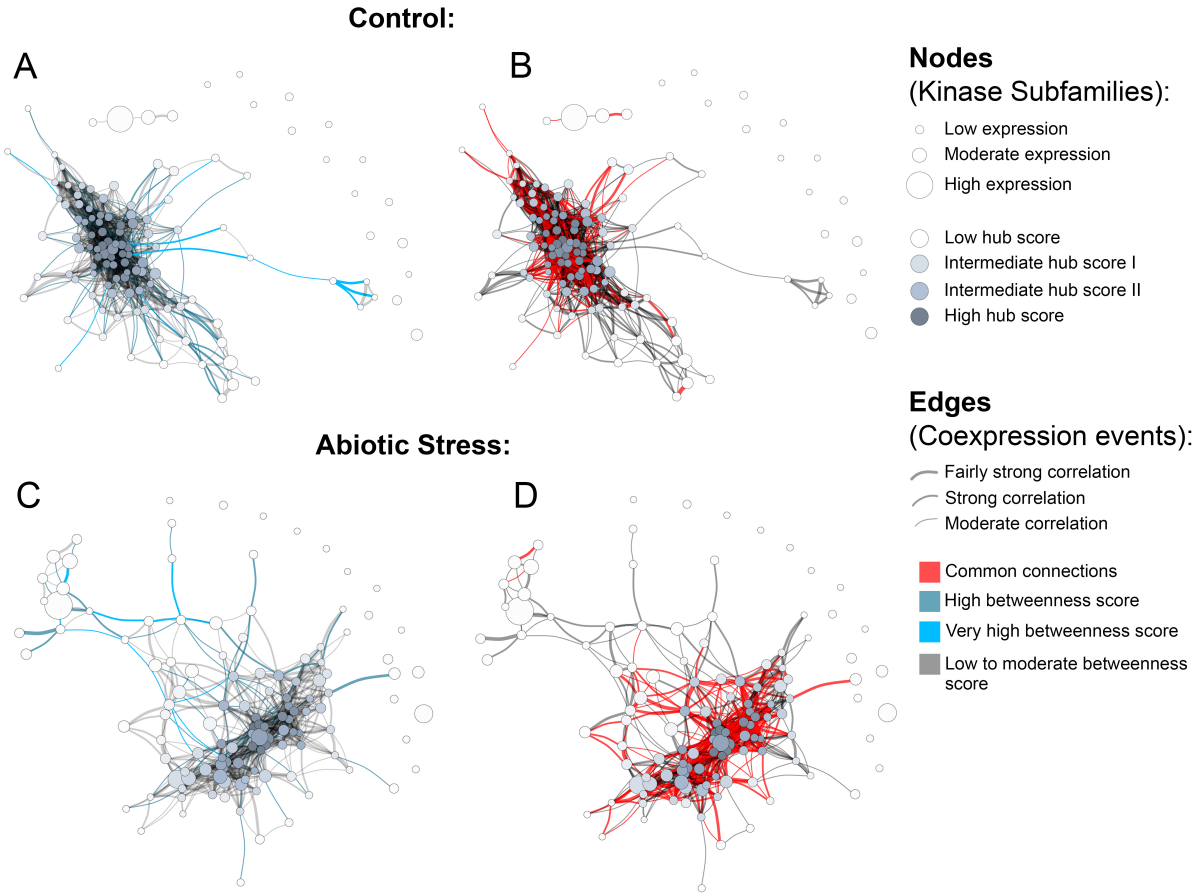

Fig. 3. Coexpression networks for *H. brasiliensis* (Hbr) kinase subfamilies. (A) Hbr control network with betweenness values highlighted in light blue. (B) Hbr control network indicating edge similarities (red) with the Hbr stress network. (C) Hbr abiotic-stress network with betweenness values highlighted in light blue. (D) Hbr abiotic stress network indicating edge similarities (red) with the Hbr control network.

To obtain an overview of the most influential subfamilies in PK processes, we first calculated hub centrality scores within each network, which are represented by the node colors in Fig. 3 (Supplementary Tables S18). Elevated hub scores (highlighted in dark gray in Fig. 3) indicated PK subfamilies with a significant number of connections. Interestingly, out of the 10 subfamilies with the highest hub scores (ranging from 0.85 to 1) in the Hbr control network, eight belonged to members of the RLK-Pelle group (RLK-Pelle_L-LEC, RLK-Pelle_RLCK-V, RLK-Pelle_RLCK-VIIa-2, RLK-Pelle_LRR-I-1, RLK-Pelle_LysM, RLK-Pelle_SD-2b, RLK-Pelle_DLSV, and RLK-Pelle_RLCK-VIIa-1), while the others were CAMK-CDPK and CK1_CK1-Pl. In contrast, under adverse conditions, the hub scores of the top

10 subfamilies varied from 0.752 to 1; only 6 of them were members of the RLK-Pelle group (RLK-Pelle_RLCK-X, RLK-Pelle_PERK-1, RLK-Pelle_LysM, RLK-Pelle_SD-2b, RLK-Pelle_L-LEC, RLK-Pelle_RLCK-VIIa-1), while the others were CAMK_CDPK, TKL-Pl-4, STE_STE7, and CK1_CK1-Pl.

Ultimately, we investigated network structural weaknesses by measuring edge betweenness centrality scores among kinase subfamily interactions (edges) within each network (Supplementary Tables S19). The edges presenting elevated betweenness values (colored in light blue in Fig. 3) indicated relationships sustained by few connections possibly related to a greater flow of interaction into the complex system modeled. Overall, under adverse conditions, PK subfamilies tended to arrange into a less cohesive network architecture, as evidenced by the large number of scattered connections. Through betweenness measures, we observed that other influential subfamily pairs of the control network were RLK-Pelle_LRR-XII-1/RLK-Pelle_RLCK-XVI, RLK-Pelle_LRR-VII-3/RLK-Pelle_RLCK-XVI, and RLK-Pelle_CR4L/RLK-Pelle_LRR-Xb-1, in contrast to the ones found during abiotic stress situations: RLK-Pelle_RLCK-Os/TKL-Pl-6, CAMK_CAMK1-DCAMKL/RLK-Pelle_RLCK-Os, and RLK-Pelle_RLCK-V/TKL-Pl-6.

4. Discussion

In the last decades, an increasing number of initiatives have been established to produce a high-quality reference genome for the rubber tree (Liu et al., 2020b; Pootakham et al., 2017; Rahman et al., 2013; Tang et al., 2016). However, the high complexity of the Hbr genome introduces many challenges that have hampered the ability to obtain contiguous genomic sequences and complete gene annotation (English et al., 2012; Pootakham et al., 2017). Although the most recent version of the Hbr genome (Liu et al., 2020b) provided the assembly of contiguous sequences for chromosomes for the first time, there is still a lack of knowledge about its gene content and functional implications, highlighting the need for efforts to profile and fully characterize important protein families, such as PKs. Here, we established a combined approach to generate a comprehensive and diverse kinase database for Hbr. Joining two independent rubber tree genomic resources (Liu et al., 2020b; Tang et al., 2016) and comparing them with kinomes from two other members of the *Euphorbiaceae* family (Mes and Rco) enabled an in-depth

investigation of the rubber tree kinome, supplying a large and reliable reservoir of data.

Plant kinomes have been studied in several other species, including 942 members in *A. thaliana* (Zulawski et al., 2014), 2,166 in soybean (Liu et al., 2015), 1,168 in grapevine (Zhang, 2003), and 1,210 in sorghum (Aono et al., 2021). In this study, we identified 2,842 PKs in the rubber tree, a considerably larger size when compared to 1,531 in cassava and 863 in castor bean. Although the rubber tree possesses a large genome (1.47 Gb), which is nearly 3-4.5 times larger than the cassava (495 Mb) and castor bean (320 Mb) genomes (Bredeson et al., 2016; Chan et al., 2010; Tang et al., 2016), the large kinome size in Hbr resulted from the combination of two sources of PKs related to different rubber tree genotypes (Reyan7-33-97 and GT1) (Liu et al., 2020b; Tang et al., 2016). When analyzing the two Hbr PK sets separately, we found a much smaller number of PKs in each of them (1,809 and 1,379), placing the Hbr kinome in the range of other plant species. The discrepancy found between the two sources of data reinforces the differences in completeness among genome assemblies that could potentially mislead further genomic investigations, especially considering the elevated heterozygosity levels and the high amount of repetitive elements in the rubber tree genome (Gouvêa et al., 2010; Lau et al., 2016). Additionally, a recent study showed that the number of PKs in sugarcane was significantly decreased on the allelic level when compared to those found for all allele copies of a given gene (Aono et al., 2021), demonstrating that the redundancy in PK datasets may contribute to the overestimation of kinome sizes.

Similar to the results of other kinome studies (Aono et al., 2021; Ferreira-Neto et al., 2021; Liu et al., 2020a, 2015; Wei et al., 2014; Yan et al., 2018; Zhu et al., 2018a; Zulawski et al., 2014), RLK-Pelle was the most pronounced group in Hbr, Mes and Rco kinomes. Considering the diverse functions of PKs (Lehti-Shiu and Shiu, 2012), the role of the group in the Hbr stress response was remarkable. One notable feature that was observed across Hbr PKs was the large diversity in domain configuration. Most PKs (56.9%) in rubber tree had two or more functional domains incorporated with them, similar to what has been observed in cassava (59.2%), castor bean (55%), soybean (56.5%) (Liu et al., 2015), and pineapple (50.7%) (Zhu et al., 2018a). Extracellular domains (ECDs) were evidenced by the following: (i) the large diversity of additional domains in PK genes; (ii) the detection of signal peptides and transmembrane regions; and (iii)

the wide range of subcellular localizations predicted (Supplementary Fig. S5). PKs combined with ECDs may broaden the scope of functionality within signaling networks by sensing new extracellular signals and their aggregation to existing response networks (Gish and Clark, 2011; Lehti-Shiu and Shiu, 2012).

Our comparative analyses of the PKs of the three *Euphorbiaceae* species revealed a high degree of similarity in their kinase subfamily compositions, protein characteristics and gene organization (Supplementary Figs. S2-S4). Our integrative approach allowed us to corroborate the validity of the Hbr kinome, which was composed of different data sources and had evident resemblances with closely related phylogenetic species. However, Mes was more similar to Hbr in kinome size than Rco. This pattern of gene expansion within the *Euphorbiaceae* clade was also observed in other gene families, including the SWEET and SBP-box families (Cao et al., 2019; Li et al., 2019). Phylogenetic studies indicated that *Hevea* and *Manihot* underwent a whole-genome duplication event before their divergence approximately 36 million years ago (MYA), while the *Ricinus* lineage diverged from other Euphorbia members approximately 60 MYA (Bredeson et al., 2016; Shearman et al., 2020). In this sense, the increase in the PK superfamily size could be partly attributed to the expansion of several gene families throughout duplication events during their evolutionary history (Lehti-Shiu and Shiu, 2012).

Indeed, our analysis suggested that segmental duplications mostly accounted for Hbr kinome expansion (Fig. 2B), with ∼58.9% of PKs displaying more than 75% compositional similarities. Tandem duplication events, on the other hand, seemed to contribute to the expansion of the PK superfamily to a lesser extent and were restricted to a few subfamilies (Supplementary Table S11), accounting for the generation of nearly 11.9% of PK genes in Hbr. This observation was within the range of what has been reported for other higher plants, such as 10.6% in soybean (Liu et al., 2015), 12.5% in pineapple (Zhu et al., 2018a), and 14.8% in strawberry (Liu et al., 2020a). Among the tandemly duplicated PKs, the most pronounced subfamilies were RLK-Pelle_DLSV, with 45 of its members associated with tandem duplication (∼16.8%). RLK-Pelle_LRR-III with 28 (∼26.2%), RLK-Pelle_LRR-XI-1 with 20 (16%), STE_STE11 with 18 (∼13.7%), and CAMK_CDPK with 12 (12.2%).

Tandemly duplicated kinases have been associated with stress responses (Freeling, 2009),

which is of great interest for molecular breeding. Additionally, in rubber tree research, different initiatives have brought to light the importance of PKs in the configuration and maintenance of economically important traits, including not only resistance to different types of stress (Duan et al., 2010; Jin et al., 2017; Mantello et al., 2019; Venkatachalam et al., 2010) but also plant performance in the field (Bini et al., 2022; Francisco et al., 2021). Together with these findings, recent contributions have pinpointed the role of TEs beyond Hbr genomic organization, suggesting a potential influence on the configuration of desirable rubber tree traits (Francisco et al., 2021; Wu et al., 2020). We also identified a considerable number of PKs (15.5%) associated with TEs.

It has been well established that TEs are abundant in the rubber tree genome, and the proportion of TE types found in our study was similar to those found by other authors (Liu et al., 2020b; Tang et al., 2016; Wu et al., 2020). Responsible for major changes in the genetic architecture (e.g., rearrangements, duplication, gene breaking, and the origin of new genes) (Bennetzen, 2005; Flagel and Wendel, 2009; Lisch, 2013), TEs are usually neutral. However, such elements possess mutagenic potential due to epigenetic mechanisms and are able to alter regulatory networks and confer genetic adaptations, leading to important phenotypic variations (Lisch, 2013; Wei and Cao, 2016; Wu et al., 2020); this has currently received great attention in genetic improvement programs for several species (Domínguez et al., 2020; Lee et al., 2006; Wang et al., 2020). In Hbr, Wu et al. (2020) showed that TEs located in gene regulatory regions in Hbr were involved in latex production through cis regulation, which would explain the differential gene expression among contrasting genotypes. The incidence of PKs close to TEs pinpoints the importance of such elements on PK functionality, as already demonstrated by other studies describing TE-mediated regulation in kinases Fan et al. (2019); Zayed et al. (2007).

Similar to PKs, which are especially active during abiotic stress (Jaggi, 2018; Morris, 2001), TEs are related to plant adaptations throughout evolution (Casacuberta and González, 2013; Dubin et al., 2018; Lisch, 2013; Naito et al., 2009; Negi et al., 2016). We found an association between TEs and specific kinase subfamilies, such as those present in the RLK-Pelle group and most abundant in the Hbr kinome. Given the important activity of this group in response

to abiotic stresses, these findings provided insights into rubber tree genetic adaptation (Zhu et al., 2018b). As expected due to the occurrence of duplication events caused by TEs (Flagel et al., 2008; Flagel and Wendel, 2009; Morgante et al., 2005), we also observed an association of these elements with tandemly duplicated PKs, enabling the elucidation of diverse biological mechanisms favoring stress resistance.

Differentially expressed gene (DEG) analyses are based on statistical tests performed on gene expression quantifications measured under certain conditions, contrasting physiological contexts and different stimuli, enabling the evaluation of increased gene expression (Casassola et al., 2013; Costa-Silva et al., 2017). Although we did not perform such an analysis of Hbr PKs due to the different experiments and datasets employed, it was possible to visualize a distinct overall expression profile for subfamily expression across the samples employed, illustrating putative molecular mechanisms adopted by PK subfamilies to overcome stress conditions (Mantello et al., 2019). The subfamilies CAMP_AMPK, CMGC_PITthe, CK1_CK1, RLK-Pelle_LRR-XIIIb, and RLK-Pelle_URK-2 exhibited more pronounced expression in samples under stress conditions, as already reported in other studies (Hawley et al., 2005; Saito et al., 2019). CAMP_AMPK has been described as an important energy regulator in eukaryotes, coordinating metabolic activities in the cytosol with those in mitochondria and plastids, possibly allocating energy expenditure to overcome these adversities (Hawley et al., 2005; Roustan et al., 2016; Suzuki et al., 2012). Although members of the CK1 subfamily were highly conserved in eukaryotes and involved in various cellular, physiological and developmental processes, their functions in plant species are still poorly understood (Saito et al., 2019). Studies indicated that CK1 members in *A. thaliana* are involved in several processes related to the response to environmental stimuli, such as regulation of stomatal opening (Zhao et al., 2016), signaling in response to blue light (Tan et al., 2013), organization and dynamics of cortical microtubules (Ben-Nissan et al., 2008), and ethylene production (Tan and Xue, 2014).

As a complementary approach to elucidate different patterns in the expression of PK subfamilies in control and abiotic stress-related samples, we employed gene coexpression networks. Through a graph representation of the PK subfamily interactions in these two different groups of samples, we estimated coexpression patterns inherent to each network, inferring functional

implications through network topology. Even with a common set of interactions (Fig. 3B and 3D), it is possible to note fewer associations in the network modeled with stress samples (a loss of ∼40%), which highlights the different molecular mechanisms of PKs under stress conditions. In a complex network structure, nodes with the largest number of connections (high degree) are called hubs, which are elements recognized as critical to network maintenance (Barabasi and Oltvai, 2004). Therefore, PK subfamilies with the highest hub scores are considered to be important regulators over the set of biological mechanisms affected by PKs (Azuaje, 2014; Barabasi and Oltvai, 2004; Van Dam et al., 2018), which provides additional insights into key mechanisms over PKs' action (Vandereyken et al., 2018).

In both networks modeled, we found that the CAMK_CDPK subfamily had the highest hub score, suggesting the importance of calcium signals over Hbr PK activities, as already reported in soybean (Liu et al., 2015). Members of the RLK-Pelle group were also identified as hubs in both networks, reinforcing the primary and secondary metabolic functions of this group (Bolhassani et al., 2021). Additionally, TKL-Pl-4 was among the hubs in the stress-related network, corroborating the already described upregulation of members of this subfamily in stress conditions (Yan et al., 2017) and reinforcing the potential of biological inferences over the network structure.

Another measure evaluated in the modeled networks was edge betweenness scores. In a complex network structure, edges with high betweenness indicate points of vulnerability in the network structure, i.e. connections that, if removed, have a larger probability of causing network separation. In the networks modeled for PK subfamily interactions, identifying such edges can identify indicators of subfamilies mediating a significant amount of mechanisms over a larger set of PKs. Different connections were identified in the networks. Interestingly, the two highest betweenness values for the control network (RLK-Pelle_LRR-XII-1/RLK-Pelle_RLCK-XVI and RLK-Pelle_LRR-VII-3/RLK-Pelle_RLCK-XVI edges) were disrupted in the stress-associated network. The RLK-Pelle_RLCK-XVI subfamily did not have any connection in the stress network, showing a change in the interaction of this subfamily under stress. RLCK members have already been shown to be related to plant growth and vegetative development (Gao and Xue, 2012; Yan et al., 2018), which is directly impacted by stress.

Additionally, in the stress-related network, we found that the PK subfamily pairs RLK-Pelle_RLCK-Os—TKL-Pl-6, CAMK_CAMK1-DCAMKL—RLK-Pelle_RLCK-Os, and RLK-Pelle_RLCK-V—TKL-Pl-6 had the largest betweenness scores. All these subfamilies presented a similar number of connections in the control network; however, they were not considered vulnerability points. This result indicated that under stress, established connections may become sensitive and cause network breaks in more adverse conditions. The interaction of RLK-Pelle_RLCK members and CAMK_CAMK1-DCAMKL and TKL-Pl-6 corroborates the previously described CAMK_CAMK1-DCAMKL induction during stress (Liu et al., 2015) and the downregulation of TKL-Pl-6 expression during stress (Yan et al., 2017).

Given the importance of rubber trees, the rising demand for latex production, and the elevated complexity of the Hbr genome (Board, 2018; Tang et al., 2016), providing resources for understanding stress responses is of great interest for Hbr breeding programs (Priyadarshan and Goncalves, 2003). Our work provided a rich and large reservoir of data for Hbr research. In the first study to profile the complete set of PKs in Hbr, we combined different data sources to provide a wider PK characterization, taking advantage of the resources available and contrasting our results with two phylogenetically close species. From a set of 2,842 PKs classified into 20 groups and distributed along all Hbr chromosomes, our findings demonstrated the high diversity and scope of functionality of Hbr PKs. Additionally, we provided different insights across stress responses in rubber trees through the association of tandemly duplicated PKs, TEs, gene expression patterns, and coexpression events.

Acknowledgements

This work was supported by grants from the Fundação de Amparo à Pesquisa do Estado de São Paulo, the Conselho Nacional de Desenvolvimento Científico e Tecnológico (CNPq) and the Coordenação de Aperfeiçoamento de Pessoal de Nível Superior (CAPES, Computational Biology Programme). LBS received an undergraduate fellowship from FAPESP (2019/19340-2); AA received a PhD fellowship from FAPESP (2019/03232-6); and FF received a PhD fellowship from FAPESP (2018/18985-7).

Author contributions

LBS, AA and FF performed all analyses and wrote the manuscript. AS, CS and LMS conceived of the project. All authors reviewed, read and approved the manuscript.

References

Altschul, S.F., Gish, W., Miller, W., Myers, E.W., Lipman, D.J., 1990. Basic local alignment search tool. J. Mol. Biol. 215, 403–410.

Andrews, S., 2010. Fastqc: a quality control tool for high throughput sequence data. version 0.11. 2. Website: http://www.bioinformatics.babraham.ac.uk/projects/fastqc.

Aono, A.H., Pimenta, R.J.G., Garcia, A.L.B., Correr, F.H., Hosaka, G.K., Carrasco, M.M., Cardoso-Silva, C.B., Mancini, M.C., Sforça, D.A., Dos Santos, L.B., et al., 2021. The wild sugarcane and sorghum kinomes: Insights into expansion, diversification, and expression patterns. Front. Plant Sci. 12, 668623.

Armenteros, J.J.A., Tsirigos, K.D., Sønderby, C.K., Petersen, T.N., Winther, O., Brunak, S., von Heijne, G., Nielsen, H., 2019. Signalp 5.0 improves signal peptide predictions using deep neural networks. Nat. Biotechnol. 37, 420–423.

Azuaje, F.J., 2014. Selecting biologically informative genes in co-expression networks with a centrality score. Biol. Direct 9, 1–23.

Barabasi, A.L., Oltvai, Z.N., 2004. Network biology: understanding the cell's functional organization. Nat. Rev. Genet. 5, 101–113.

Ben-Nissan, G., Cui, W., Kim, D.J., Yang, Y., Yoo, B.C., Lee, J.Y., 2008. Arabidopsis casein kinase 1-like 6 contains a microtubule-binding domain and affects the organization of cortical microtubules. Plant Physiol. 148, 1897–1907.

Bennetzen, J.L., 2005. Transposable elements, gene creation and genome rearrangement in flowering plants. Curr. Opin. Genet. Dev. 15, 621–627.

512 Bini, K., Saha, T., Radhakrishnan, S., Ravindran, M., Uthup, T.K., 2022. Development of
513 novel markers for yield in Hevea brasiliensis Muell. Arg. based on candidate genes from
514 biosynthetic pathways associated with latex production. Biochem. Genet., 1–29.

515 Board, M.R., 2018. Natural rubber statistics 2018. (Kuala Lumpur: Malaysian Rubber Board).

516 Bolger, A.M., Lohse, M., Usadel, B., 2014. Trimmomatic: a flexible trimmer for illumina
517 sequence data. Bioinformatics 30, 2114–2120.

518 Bolhassani, M., Niazi, A., Tahmasebi, A., Moghadam, A., 2021. Identification of key genes
519 associated with secondary metabolites biosynthesis by system network analysis in valeriana
520 officinalis. J. Plant Res. 134, 625–639.

521 Brandes, U., 2001. A faster algorithm for betweenness centrality. J. Math. Soc. 25, 163–177.

522 Bredeson, J.V., Lyons, J.B., Prochnik, S.E., Wu, G.A., Ha, C.M., Edsinger-Gonzales, E.,
523 Grimwood, J., Schmutz, J., Rabbi, I.Y., Egesi, C., et al., 2016. Sequencing wild and cultivated
524 cassava and related species reveals extensive interspecific hybridization and genetic diversity.
525 Nat. Biotechnol. 34, 562–570.

526 Cao, Y., Liu, W., Zhao, Q., Long, H., Li, Z., Liu, M., Zhou, X., Zhang, L., 2019. Integra-
527 tive analysis reveals evolutionary patterns and potential functions of sweet transporters in
528 Euphorbiaceae. Int. J. Biol. Macromol. 139, 1–11.

529 Casacuberta, E., González, J., 2013. The impact of transposable elements in environmental
530 adaptation. Mol. Ecol. 22, 1503–1517.

531 Casassola, A., Brammer, S.P., Chaves, M.S., Martinelli, J.A., Grando, M.F., Denardin, N.,
532 2013. Gene expression: a review on methods for the study of defense-related gene differential
533 expression in plants.

534 Chan, A.P., Crabtree, J., Zhao, Q., Lorenzi, H., Orvis, J., Puiu, D., Melake-Berhan, A., Jones,
535 K.M., Redman, J., Chen, G., et al., 2010. Draft genome sequence of the oilseed species
536 ricinus communis. Nat. Biotechnol. 28, 951–956.

Cheng, H., Chen, X., Fang, J., An, Z., Hu, Y., Huang, H., 2018. Comparative transcriptome analysis reveals an early gene expression profile that contributes to cold resistance in hevea brasiliensis (the para rubber tree). Tree Physiol. 38, 1409–1423.

Colcombet, J., Hirt, H., 2008. Arabidopsis MAPKs: a complex signalling network involved in multiple biological processes. Biochem. J. 413, 217–226.

Conesa, A., Götz, S., 2008. Blast2GO: a comprehensive suite for functional analysis in plant genomics. Int. J. Plant Genomics 2008.

Consortium, U., 2019. Uniprot: a worldwide hub of protein knowledge. Nucleic Acids Res. 47, D506–D515.

Costa-Silva, J., Domingues, D., Lopes, F.M., 2017. Rna-seq differential expression analysis: An extended review and a software tool. PLoS One 12, e0190152.

Csardi, G., Nepusz, T., et al., 2006. The igraph software package for complex network research. Int. J. Complex Syst. 1695, 1–9.

Deng, X., Wang, J., Li, Y., Wu, S., Yang, S., Chao, J., Chen, Y., Zhang, S., Shi, M., Tian, W., 2018. Comparative transcriptome analysis reveals phytohormone signalings, heat shock module and ROS scavenger mediate the cold-tolerance of rubber tree. Sci. Rep. 8, 1–16.

Devakumar, A., Prakash, P.G., Sathik, M., Jacob, J., 1999. Drought alters the canopy architecture and micro-climate of hevea brasiliensis trees. Trees 13, 161–167.

Devakumar, A., Sathik, M.M., Sreelatha, S., Thapliyal, A., Jacob, J., 2002. Photosynthesis in mature trees of hevea brasiliensis experiencing drought and cold stresses concomitant with high light in the field. Indian J. Nat. Rubb. Res. 15, 1–13.

Domínguez, M., Dugas, E., Benchouaia, M., Leduque, B., Jiménez-Gómez, J.M., Colot, V., Quadrana, L., 2020. The impact of transposable elements on tomato diversity. Nat. Commun. 11, 1–11.

561 Duan, C., Rio, M., Leclercq, J., Bonnot, F., Oliver, G., Montoro, P., 2010. Gene expres-
562 sion pattern in response to wounding, methyl jasmonate and ethylene in the bark of hevea
563 brasiliensis. Tree Physiol. 30, 1349–1359.

564 Dubin, M.J., Scheid, O.M., Becker, C., 2018. Transposons: a blessing curse. Curr. Opin. Plant
565 Biol. 42, 23–29.

566 Edgar, R.C., 2004. Muscle: multiple sequence alignment with high accuracy and high through-
567 put. Nucleic Acids Res. 32, 1792–1797.

568 El-Gebali, S., Mistry, J., Bateman, A., Eddy, S.R., Luciani, A., Potter, S.C., Qureshi, M.,
569 Richardson, L.J., Salazar, G.A., Smart, A., et al., 2019. The pfam protein families database
570 in 2019. Nucleic Acids Res. 47, D427–D432.

571 English, A.C., Richards, S., Han, Y., Wang, M., Vee, V., Qu, J., Qin, X., Muzny, D.M., Reid,
572 J.G., Worley, K.C., et al., 2012. Mind the gap: upgrading genomes with pacific biosciences
573 RS long-read sequencing technology. PLoS One 7, e47768.

574 Fan, Y., Bazai, S.K., Daian, F., Arechederra, M., Richelme, S., Temiz, N.A., Yim, A., Haber-
575 mann, B.H., Dono, R., Largaespada, D.A., et al., 2019. Evaluating the landscape of gene
576 cooperativity with receptor tyrosine kinases in liver tumorigenesis using transposon-mediated
577 mutagenesis. J. Hepatol. 70, 470–482.

578 Ferreira-Neto, J.R.C., Borges, A.N.d.C., da Silva, M.D., Morais, D.A.d.L., Bezerra-Neto, J.P.,
579 Bourque, G., Kido, E.A., Benko-Iseppon, A.M., 2021. The cowpea kinome: Genomic and
580 transcriptomic analysis under biotic and abiotic stresses. Front. Plant Sci. , 945.

581 Finn, R.D., Clements, J., Eddy, S.R., 2011. Hmmer web server: interactive sequence similarity
582 searching. Nucleic Acids Res. 39, W29–W37.

583 Flagel, L., Udall, J., Nettleton, D., Wendel, J., 2008. Duplicate gene expression in allopolyploid
584 gossypium reveals two temporally distinct phases of expression evolution. BMC Biol. 6, 1–9.

585 Flagel, L.E., Wendel, J.F., 2009. Gene duplication and evolutionary novelty in plants. New
586 Phytol. 183, 557–564.

587 Francisco, F.R., Aono, A.H., Da Silva, C.C., Gonçalves, P.S., Junior, E.J.S., Le Guen, V.,
588 Fritsche-Neto, R., Souza, L.M., de Souza, A.P., 2021. Unravelling rubber tree growth by
589 integrating GWAS and biological network-based approaches. Front. Plant Sci. 12.

590 Freeling, M., 2009. Bias in plant gene content following different sorts of duplication: tandem,
591 whole-genome, segmental, or by transposition. Annu. Rev. Plant Biol. 60, 433–453.

592 Fu, L., Niu, B., Zhu, Z., Wu, S., Li, W., 2012. CD-HIT: accelerated for clustering the next-
593 generation sequencing data. Bioinformatics 28, 3150–3152.

594 Gao, L.L., Xue, H.W., 2012. Global analysis of expression profiles of rice receptor-like kinase
595 genes. Mol. Plant 5, 143–153.

596 Gasteiger, E., Gattiker, A., Hoogland, C., Ivanyi, I., Appel, R.D., Bairoch, A., 2003. Expasy:
597 the proteomics server for in-depth protein knowledge and analysis. Nucl. Acids Res. 31,
598 3784–3788.

599 Geer, L.Y., Marchler-Bauer, A., Geer, R.C., Han, L., He, J., He, S., Liu, C., Shi, W., Bryant,
600 S.H., 2010. The NCBI biosystems database. Nucleic Acids Res. 38, D492–D496.

601 Gish, L.A., Clark, S.E., 2011. The RLK/pelle family of kinases. Plant J. 66, 117–127.

602 Goodstein, D.M., Shu, S., Howson, R., Neupane, R., Hayes, R.D., Fazo, J., Mitros, T., Dirks,
603 W., Hellsten, U., Putnam, N., et al., 2012. Phytozome: a comparative platform for green
604 plant genomics. Nucleic Acids Res. 40, D1178–D1186.

605 Gouvêa, L.R.L., Rubiano, L.B., Chioratto, A.F., Zucchi, M.I., Gonçalves, P.d.S., 2010. Genetic
606 divergence of rubber tree estimated by multivariate techniques and microsatellite markers.
607 Genet. Mol. Biol. 33, 308–318.

608 Guo, D., Li, H.L., Zhu, J.H., Wang, Y., An, F., Xie, G.S., Peng, S.Q., 2017. Genome-wide
609 identification, characterization, and expression analysis of SnRK2 family in hevea brasiliensis.
610 Tree Genet. Genomes 13, 1–12.

611 Hawley, S.A., Pan, D.A., Mustard, K.J., Ross, L., Bain, J., Edelman, A.M., Frenguelli, B.G.,
612 Hardie, D.G., 2005. Calmodulin-dependent protein kinase kinase-β is an alternative upstream
613 kinase for amp-activated protein kinase. Cell Metab. 2, 9–19.

614 Hoa, T., Tuy, L., Duong, P., Phuc, L., Truong, V., 1998. Selection of hevea clones for the
615 1998–2000 planting recommendation in Vietnam, in: Proc. IRRDB Symposium on Natural
616 Rubber, pp. 164–177.

617 Hora Júnior, B.T.d., de Macedo, D.M., Barreto, R.W., Evans, H.C., Mattos, C.R.R., Maffia,
618 L.A., Mizubuti, E.S., 2014. Erasing the past: a new identity for the damoclean pathogen
619 causing south American leaf blight of rubber. PLoS One 9, e104750.

620 Ihaka, R., Gentleman, R., 1996. R: a language for data analysis and graphics. J. Comput.
621 Graph. Stat. 5, 299–314.

622 Jaggi, M., 2018. Recent advancement on map kinase cascade in biotic stress, in: Molecular
623 Aspects of Plant-Pathogen Interaction. Springer, New York, pp. 139–158.

624 Jin, X., Zhu, L., Yao, Q., Meng, X., Ding, G., Wang, D., Xie, Q., Tong, Z., Tao, C., Yu,
625 L., et al., 2017. Expression profiling of mitogen-activated protein kinase genes reveals their
626 evolutionary and functional diversity in different rubber tree (hevea brasiliensis) cultivars.
627 Genes 8, 261.

628 Kleinberg, J.M., 1999. Hubs, authorities, and communities. ACM Comput. Surv. (CSUR) 31,
629 5–es.

630 Kolde, R., Kolde, M.R., 2015. Package "pheatmap". R Package 1, 790.

631 Kovtun, Y., Chiu, W.L., Tena, G., Sheen, J., 2000. Functional analysis of oxidative stress-
632 activated mitogen-activated protein kinase cascade in plants. Proc. Natl. Acad. Sci. 97,
633 2940–2945.

634 Krogh, A., Larsson, B., Von Heijne, G., Sonnhammer, E.L., 2001. Predicting transmembrane
635 protein topology with a hidden Markov model: application to complete genomes. J. Mol.
636 Biol. 305, 567–580.

637 Krzywinski, M., Schein, J., Birol, I., Connors, J., Gascoyne, R., Horsman, D., Jones, S.J.,
638 Marra, M.A., 2009. Circos: an information aesthetic for comparative Genomics. Genome
639 Res. 19, 1639–1645.

640 Kunjet, S., Thaler, P., Gay, F., Chuntuma, P., Sangkhasila, K., Kasemsap, P., 2013. Effects
641 of drought and tapping for latex production on water relations of hevea brasiliensis trees.
642 Agric. Nat. Resour. 47, 506–515.

643 Kuruvilla, L., Sathik, M.M., Thomas, M., Luke, L.P., Sumesh, K., 2017. Identification and val-
644 idation of cold responsive micrornas of hevea brasiliensis using high throughput sequencing.
645 J. Crop Sci. Biotechnol. 20, 369–377.

646 Lau, N.S., Makita, Y., Kawashima, M., Taylor, T.D., Kondo, S., Othman, A.S., Shu-Chien,
647 A.C., Matsui, M., 2016. The rubber tree genome shows expansion of gene family associated
648 with rubber biosynthesis. Sci. Rep. 6, 1–14.

649 Lee, J.K., Park, J.Y., Kim, J.H., Kwon, S.J., Shin, J.H., Hong, S.K., Min, H.K., Kim, N.S.,
650 2006. Genetic mapping of the Isaac-CACTA transposon in maize. Theor. Appl. Genet. 113,
651 16–22.

652 Lehti-Shiu, M.D., Shiu, S.H., 2012. Diversity, classification and function of the plant protein
653 kinase superfamily. Philos. Trans. R. Soc. B: Biol. Sci. 367, 2619–2639.

654 Leinonen, R., Sugawara, H., Shumway, M., Collaboration, I.N.S.D., 2010. The sequence read
655 archive. Nucleic Acids Res. 39, D19–D21.

656 Li, D., Zeng, R., Li, Y., Zhao, M., Chao, J., Li, Y., Wang, K., Zhu, L., Tian, W.M., Liang, C.,
657 2016. Gene expression analysis and snp/indel discovery to investigate yield heterosis of two
658 rubber tree f1 hybrids. Sci. Rep. 6, 1–12.

659 Li, J., Gao, X., Sang, S., Liu, C., 2019. Genome-wide identification, phylogeny, and expression
660 analysis of the SBP-box gene family in Euphorbiaceae. BMC Genom. 20, 1–15.

661 Lisch, D., 2013. How important are transposons for plant evolution? Nat. Rev. Genet. 14,
662 49–61.

663 Liu, H., Qu, W., Zhu, K., Cheng, Z.M.M., 2020a. The wild strawberry kinome: identification,
664 classification and transcript profiling of protein kinases during development and in response
665 to gray mold infection. BMC Genom. 21, 1–14.

666 Liu, J., Chen, N., Grant, J.N., Cheng, Z.M., Stewart Jr, C.N., Hewezi, T., 2015. Soybean
667 kinome: functional classification and gene expression patterns. J. Exp. Bot. 66, 1919–1934.

668 Liu, J., Shi, C., Shi, C.C., Li, W., Zhang, Q.J., Zhang, Y., Li, K., Lu, H.F., Shi, C., Zhu, S.T.,
669 et al., 2020b. The chromosome-based rubber tree genome provides new insights into spurge
670 genome evolution and rubber biosynthesis. Mol. Plant 13, 336–350.

671 Mantello, C.C., Boatwright, L., da Silva, C.C., Scaloppi, E.J., de Souza Goncalves, P., Bar-
672 bazuk, W.B., de Souza, A.P., 2019. Deep expression analysis reveals distinct cold-response
673 strategies in rubber tree (hevea brasiliensis). BMC Genom. 20, 1–20.

674 Meti, S., Meenattoor, J., Mondal, G., Chaudhuri, D., 2003. Impact of cold weather condition
675 on the growth of hevea brasiliensis clones in northern west bengal. Indian J. Nat. Rubber
676 Res. 16, 53–59.

677 Miller, M.A., Pfeiffer, W., Schwartz, T., 2011. The cipres science gateway: a community
678 resource for phylogenetic analyses, in: Proceedings of the 2011 TeraGrid Conference: Extreme
679 Digital Discovery, pp. 1–8.

680 Montoro, P., Wu, S., Favreau, B., Herlinawati, E., Labrune, C., Martin-Magniette, M.L.,
681 Pointet, S., Rio, M., Leclercq, J., Ismawanto, S., et al., 2018. Transcriptome analysis in
682 hevea brasiliensis latex revealed changes in hormone signalling pathways during ethephon
683 stimulation and consequent tapping panel dryness. Sci. Rep. 8, 1–12.

684 Morgante, M., Brunner, S., Pea, G., Fengler, K., Zuccolo, A., Rafalski, A., 2005. Gene duplica-
685 tion and exon shuffling by helitron-like transposons generate intraspecies diversity in maize.
686 Nat. Genet. 37, 997–1002.

687 Morris, P.C., 2001. Map kinase signal transduction pathways in plants. New Phytol. 151, 67–89.

688 Naito, K., Zhang, F., Tsukiyama, T., Saito, H., Hancock, C.N., Richardson, A.O., Okumoto,
689 Y., Tanisaka, T., Wessler, S.R., 2009. Unexpected consequences of a sudden and massive
690 transposon amplification on rice gene expression. Nature 461, 1130–1134.

691 Negi, P., Rai, A.N., Suprasanna, P., 2016. Moving through the stressed genome: emerging
692 regulatory roles for transposons in plant stress response. Front. Plant Sci. 7, 1448.

693 Patro, R., Duggal, G., Love, M.I., Irizarry, R.A., Kingsford, C., 2017. Salmon provides fast
694 and bias-aware quantification of transcript expression. Nat. Methods 14, 417–419.

695 Pedro, D.L.F., Lorenzetti, A.P.R., Domingues, D.S., Paschoal, A.R., 2018. PlaNC-TE: a com-
696 prehensive knowledgebase of non-coding RNAs and transposable elements in plants. Database
697 2018.

698 Pootakham, W., Sonthirod, C., Naktang, C., Ruang-Areerate, P., Yoocha, T., Sangsrakru, D.,
699 Theerawattanasuk, K., Rattanawong, R., Lekawipat, N., Tangphatsornruang, S., 2017. De
700 novo hybrid assembly of the rubber tree genome reveals evidence of paleotetraploidy in hevea
701 species. Sci. Rep. 7, 1–15.

702 Price, M.N., Dehal, P.S., Arkin, A.P., 2010. Fasttree 2–approximately maximum-likelihood
703 trees for large alignments. PLoS One 5, e9490.

704 Priyadarshan, P., Goncalves, P.d.S., 2003. Hevea gene pool for breeding. Genet. Resour. Crop
705 Evol. 50, 101–114.

706 Pushparajah, E., 1983. Problems and potentials for establishing hevea under difficult environ-
707 mental conditions. Planter.

708 Rahman, A.Y.A., Usharraj, A.O., Misra, B.B., Thottathil, G.P., Jayasekaran, K., Feng, Y.,
709 Hou, S., Ong, S.Y., Ng, F.L., Lee, L.S., et al., 2013. Draft genome sequence of the rubber
710 tree hevea brasiliensis. BMC Genom. 14, 1–15.

711 Rahman, S.N.A., Bakar, M.F.A., Singham, G.V., Othman, A.S., 2019. Single-nucleotide poly-
712 morphism markers within MVA and MEP pathways among hevea brasiliensis clones through
713 transcriptomic analysis. 3 Biotech 9, 1–10.

714 Roustan, V., Jain, A., Teige, M., Ebersberger, I., Weckwerth, W., 2016. An evolutionary
715 perspective of AMPK–TOR signaling in the three domains of life. J. Exp. Bot. 67, 3897–
716 3907.

717 Saito, A.N., Matsuo, H., Kuwata, K., Ono, A., Kinoshita, T., Yamaguchi, J., Nakamichi, N.,
718 2019. Structure–function study of a novel inhibitor of the casein kinase 1 family in arabidopsis
719 thaliana. Plant Direct 3, e00172.

720 Sathik, M.M., Luke, L.P., Rajamani, A., Kuruvilla, L., Sumesh, K., Thomas, M., 2018. De
721 novo transcriptome analysis of abiotic stress-responsive transcripts of hevea brasiliensis. Mol.
722 Breed. 38, 1–17.

723 Sevillano, L., Sanchez-Ballesta, M.T., Romojaro, F., Flores, F.B., 2009. Physiological, hor-
724 monal and molecular mechanisms regulating chilling injury in horticultural species. posthar-
725 vest technologies applied to reduce its impact. J. Sci. Food Agric. 89, 555–573.

726 Shearman, J.R., Pootakham, W., Tangphatsornruang, S., 2020. The bpm 24 rubber tree
727 genome, organellar genomes and synteny within the family euphorbiaceae. Rubber Tree
728 Genome 55.

729 Sperschneider, J., Catanzariti, A.M., DeBoer, K., Petre, B., Gardiner, D.M., Singh, K.B.,
730 Dodds, P.N., Taylor, J.M., 2017. Localizer: subcellular localization prediction of both plant
731 and effector proteins in the plant cell. Sci. Rep. 7, 1–14.

732 Suzuki, N., Koussevitzky, S., Mittler, R., Miller, G., 2012. ROS and redox signalling in the
733 response of plants to abiotic stress. Plant Cell Environ. 35, 259–270.

734 Tan, D., Hu, X., Fu, L., Kumpeangkeaw, A., Ding, Z., Sun, X., Zhang, J., 2017. Compar-
735 ative morphology and transcriptome analysis reveals distinct functions of the primary and
736 secondary laticifer cells in the rubber tree. Sci. Rep. 7, 1–17.

737 Tan, S.T., Dai, C., Liu, H.T., Xue, H.W., 2013. Arabidopsis casein kinase1 proteins CK1. 3
738 and CK1. 4 phosphorylate cryptochrome2 to regulate blue light signaling. Plant Cell 25,
739 2618–2632.

740 Tan, S.T., Xue, H.W., 2014. Casein kinase 1 regulates ethylene synthesis by phosphorylating
741 and promoting the turnover of acs5. Cell Rep. 9, 1692–1702.

742 Tang, C., Yang, M., Fang, Y., Luo, Y., Gao, S., Xiao, X., An, Z., Zhou, B., Zhang, B., Tan,
743 X., et al., 2016. The rubber tree genome reveals new insights into rubber production and
744 species adaptation. Nat. Plants 2, 1–10.

745 Van Dam, S., Vosa, U., van der Graaf, A., Franke, L., de Magalhaes, J.P., 2018. Gene co-
746 expression analysis for functional classification and gene–disease predictions. Brief. Bioinfor-
747 matics 19, 575–592.

748 Vandereyken, K., Van Leene, J., De Coninck, B., Cammue, B.P., 2018. Hub protein controversy:
749 taking a closer look at plant stress response hubs. Front. Plant Sci. 9, 694.

750 Venkatachalam, P., Geetha, N., Priya, P., Thulaseedharan, A., 2010. Identification of a differ-
751 entially expressed thymidine kinase gene related to tapping panel dryness syndrome in the
752 rubber tree (hevea brasiliensis muell. arg.) by random amplified polymorphic dna screening.
753 Int. J. Plant Biol. 1, e7.

754 Villanueva, R.A.M., Chen, Z.J., 2019. ggplot2: elegant graphics for data analysis.

755 Voorrips, R., 2002. Mapchart: software for the graphical presentation of linkage maps and
756 QTLs. J. Hered. 93, 77–78.

757 Wang, J., Lu, N., Yi, F., Xiao, Y., 2020. Identification of transposable elements in conifer and
758 their potential application in breeding. Evol. Bioinform. 16, 1176934320930263.

759 Wei, K., Wang, Y., Xie, D., 2014. Identification and expression profile analysis of the protein
760 kinase gene superfamily in maize development. Mol. Breed. 33, 155–172.

761 Wei, L., Cao, X., 2016. The effect of transposable elements on phenotypic variation: insights
762 from plants to humans. Sci. China Life Sci. 59, 24–37.

763 Wu, S., Guyot, R., Bocs, S., Droc, G., Oktavia, F., Hu, S., Tang, C., Montoro, P., Leclercq,
764 J., 2020. Structural and functional annotation of transposable elements revealed a potential

765 regulation of genes involved in rubber biosynthesis by TE-Derived siRNA interference in
766 Hevea brasiliensis. Int. J. Mol. Sci. 21, 4220.

767 Xiao, X.H., Yang, M., Sui, J.L., Qi, J.Y., Fang, Y.J., Hu, S.N., Tang, C.R., 2017. The
768 calcium-dependent protein kinase (CDPK) and CDPK-related kinase gene families in hevea
769 brasiliensis–comparison with five other plant species in structure, evolution, and expression.
770 FEBS Open Bio 7, 4–24.

771 Yan, J., Li, G., Guo, X., Li, Y., Cao, X., 2018. Genome-wide classification, evolutionary
772 analysis and gene expression patterns of the kinome in gossypium. PLoS One 13, e0197392.

773 Yan, J., Su, P., Wei, Z., Nevo, E., Kong, L., 2017. Genome-wide identification, classification,
774 evolutionary analysis and gene expression patterns of the protein kinase gene family in wheat
775 and Aegilops tauschii. Plant Mol. Biol. 95, 227–242.

776 Yu, C.S., Chen, Y.C., Lu, C.H., Hwang, J.K., 2006. Prediction of protein subcellular localiza-
777 tion. Proteins: Struct. Funct. Bioinform. 64, 643–651.

778 Yu, G., Smith, D.K., Zhu, H., Guan, Y., Lam, T.T.Y., 2017. ggtree: an r package for visual-
779 ization and annotation of phylogenetic trees with their covariates and other associated data.
780 Methods Ecol. Evol. 8, 28–36.

781 Zayed, H., Xia, L., Yerich, A., Yant, S.R., Kay, M.A., Puttaraju, M., McGarrity, G.J., Wiest,
782 D.L., McIvor, R.S., Tolar, J., et al., 2007. Correction of dna protein kinase deficiency by
783 spliceosome-mediated rna trans-splicing and sleeping beauty transposon delivery. Mol. Ther.
784 15, 1273–1279.

785 Zhang, J., 2003. Evolution by gene duplication: an update. Trends in ecology & evolution 18,
786 292–298.

787 Zhao, S., Jiang, Y., Zhao, Y., Huang, S., Yuan, M., Zhao, Y., Guo, Y., 2016. Casein kinase1-
788 like protein2 regulates actin filament stability and stomatal closure via phosphorylation of
789 actin depolymerizing factor. The Plant Cell 28, 1422–1439.

Zhu, K., Liu, H., Chen, X., Cheng, Q., Cheng, Z.M.M., 2018a. The kinome of pineapple: catalog and insights into functions in crassulacean acid metabolism plants. BMC plant Biol. 18, 1–16.

Zhu, L., Jin, X., Xie, Q., Yao, Q., Wang, X., Li, H., 2018b. Calcium-dependent protein kinase family genes involved in ethylene-induced natural rubber production in different hevea brasiliensis cultivars. Int. J. Mol. Sci. 19, 947.

Zulawski, M., Schulze, G., Braginets, R., Hartmann, S., Schulze, W.X., 2014. The arabidopsis kinome: phylogeny and evolutionary insights into functional diversification. BMC Genom. 15, 1–15.

Supplementary Tables

Table S1a. Kinase domain annotation of 3,188 *H. brasiliensis* protein kinases.

Table S1b. Kinase domain annotation of 1,531 *M. esculenta* protein kinases.

Table S1c. Kinase domain annotation of 863 *R. communis* protein kinases.

Table S2a. *H. brasiliensis* kinase domain organization of 191 protein kinases containing multiple kinase domains.

Table S2b. *M. esculenta* kinase domain organization of 91 protein kinases containing multiple kinase domains.

Table S2c. *R. communis* kinase domain organization of 44 protein kinases containing multiple kinase domains.

Table S3a. Subfamily classification of *H. brasiliensis* protein kinases.

Table S3b. Subfamily classification of *M. esculenta* protein kinases.

Table S3c. Subfamily classification of *R. communis* protein kinases.

Table S4. The number of kinase genes in different subfamilies.

Table S5a. Characterization of *H. brasiliensis* protein kinases.

Table S5b. Characterization of *M. esculenta* protein kinases.

Table S5c. Characterization of *R. communis* protein kinases.

Table S6a. *H. brasiliensis* 2,842 kinase gene localizations and intron quantities.

Table S6b. *M. esculenta* 1,531 kinase gene localizations and intron quantities.

Table S6c. *R. communis* 863 kinase gene localizations and intron quantities.

Table S7. Chromosomal position estimation of 1,636 *H. brasiliensis* kinase genes.

Table S8a. Gene Ontology (GO) annotations for the 2,842 *H. brasiliensis* protein kinases.

Table S8b. Gene Ontology (GO) annotations for the 1,531 *M. esculenta* protein kinases.

Table S8c. Gene Ontology (GO) annotations for the 863 *R. communis* protein kinases.

Table S9a. Domain annotation of *H. brasiliensis* protein kinases.

Table S9b. Domain annotation of *M. esculenta* protein kinases.

Table S9c. Domain annotation of *R. communis* protein kinases.

Table S10a. Domain organization of *H. brasiliensis* protein kinases.

Table S10b. Domain organization of *M. esculenta* protein kinases.

Table S10c. Domain organization of *R. communis* protein kinases.

Table S11. Tandemly duplicated kinase genes across the *H. brasiliensis* genome.

Table S12. Pairs of tandemly duplicated kinases correspondences in the *H. brasiliensis* genome.

Table S13. Number of *H. brasiliensis* protein kinases near transposable elements.

Table S14. Description of *H. brasiliensis* kinase genes associated with transposable elements.

Table S15. *H. brasiliensis* RNA-Seq experiment organization (retrieved from the SRA database).

Table S16. *H. brasiliensis* kinase transcripts per million (TPM) values across samples.

Table S17. *H. brasiliensis* kinase quantifications across subfamilies.

Table S18a. Related information of the *H. brasiliensis* kinase subfamily control coexpression network.

Table S18b. Related information of the *H. brasiliensis* kinase subfamily stress coexpression network.

Table S19a. Edge betweenness values calculated across the *H. brasiliensis* kinase subfamily control network.

Table S19b. Edge betweenness values calculated across the *H. brasiliensis* kinase subfamily stress network.

Supplementary Figures

Fig. S1. Phylogenetic analysis of 2,842 *H. brasiliensis* putative typical kinase proteins with 1,000 bootstrap replicates. Each protein is represented by a unique branch tip, and branch colors represent the kinase subfamily classification.

Fig. S2. Phylogenetic analysis of 2,842 *H. brasiliensis*, 1,531 *M. esculenta*, and 863 *R. communis* putative typical kinase proteins with 1,000 bootstrap replicates. Each protein is represented by a unique branch tip, and branch colors represent the kinase subfamily classification.

Fig. S3. Chromosomal positions of (A) 2,842 PK genes identified in *H. brasiliensis* and 1,531 PK genes identified in *M. esculenta*.

Fig. S4. (A) Molecular weight and (B) isoelectric point (pI) distribution of *H. brasiliensis* (Hbr), *M. esculenta* (Mes), and *R. communis* (Rco) protein kinases.

Fig. S5. Subcellular localization predictions of (1) *H. brasiliensis*, (2) *M. esculenta*, and (3) *R. communis* protein kinases using LOCALIZER software (A), CELLO software (B), and Gene Ontology terms (C).

Fig. S6. Gene Ontology (GO) categories (biological process) of 339 tandemly duplicated *H. brasiliensis* protein kinases.

Fig. S7. Gene Ontology (GO) categories (biological process) of (A) 2,842 *H. brasiliensis* protein kinases (PKs), (B) 1,531 *M. esculenta* PKs, and (C) 863 *R. communis* PKs.

Fig. S8. RNA expression profiles of *H. brasiliensis* protein kinases among 42 samples under control conditions. Sample IDs (columns) and subfamily names (rows) were clustered based on Euclidean distances.

Fig. S9. RNA expression profiles of *H. brasiliensis* protein kinases among 37 samples under abiotic stress conditions (cold, drought, jasmonate and ethylene treatments). Sample IDs (bottom) and subfamily names (right) were clustered based on Euclidean distances.

Fig. S10. RNA expression profiles of *H. brasiliensis* PKs among all 79 samples under control and stress conditions.